ISSN: 2634 - 8853

Journal of Engineering and Applied Sciences Technology

SCIENTIFIC Research and Community

Research Article

Open Access

Role of Artificial Aggregates of Fly Ash and Slag Concretes At Different Water-To-Cement Ratios in Mechanical and Permeability Behavior

Samadar S Majeed

Architectural Department College of Engineering, Nawroz University, Iraq

ABSTRACT

This study presents an experimental investigation on the effect of artificial aggregate utilization fracture and permeability properties of concretes. For this, two types of artificial aggregates, namely, artificial fly ash aggregate (AFA) from cold bonding agglomeration process of fly ash and Portland cement and artificial slag aggregate (ASA) from cold bonding agglomeration process of ground granulated blast furnace slag and Portland cement, were replaced with natural aggregate as coarse aggregate. Moreover, to investigate the influence of water-to-cement ratio, three different water-to-cement ratios of 0.35, 0.45, and 0.55 were considered in the concrete production. The concretes were tested for the mechanical property in terms of as compressive strength, modulus of elasticity, and splitting, net flexural strength, and fracture energy and also permeability property such as water sorptivity, water penetration, gas permeability, and resistance to chloride ion penetration. The test results were also analyzed by means of statistical technique, namely, GLM-ANOVA. It was found that the use of cold bonded fly ash and slag aggregates were very effective on the performance characteristics of concretes depending on w/c ratio.

***Corresponding author**

Samadar S Majeed, Architectural Department College of Engineering, Nawroz University, Iraq. E-mail: Samadar7090@gmail.com

Received: February 17, 2021; **Accepted:** February 22, 2021; **Published:** March 04, 2021

Keywords: Recycling, Mechanical properties, Fracture, permeability properties

Introduction

Concrete is the most widely used construction material all around the world since it has superior properties such as excellent versatility, availability, and economy compared to other structural materials. However, the utilization of concrete in some structures is limited due to its high unit weight and lo w tensile strength compared to compressive strength. The development in concrete technology offers to decrease the self weight of concrete with utilization of lightweight aggregate instead of normal weight aggregate which affecting the some properties of concrete such as the workability, strength, dimensional stability, and durability as well as the cost of concrete [1,2].

Concrete with lightweight aggregates has been used successfully for structural purposes since the second half of the twentieth century, and became a very proper alternative when compared with conventional concrete. Expanded clay or shale, and sintered fly ash, which are commercially available lightweight aggregates, are acquired through heat treatment at 1000-1200 °C [3]. The agglomeration of some waste powder materials such as fly ash (FA) and ground granulated blast furnace slag (GGBFS) by cold bonding process is an alternative way of producing lightweight aggregate with an environmental impact and minimum energy consumption. Lime or Portland cement (PC) is used as binder and the water is wetting agent acting as coagulant so that the moist mixture would be pelletized in a tilted revolving pan. Large amount of FA and GGBFS is produced by industries in Turkey. Like most of the other industrialized countries, Turkey produces 15 million tons of FA and 600,000 tons of GGBFS per year and only limited amounts of them are utilized in the construction industry [4,5]. For this reason, using of FA and GGBFS in the manufacturing of lightweight aggregate may be a feasible way for recycling of such waste materials by using any technique of production such as sintering, autoclaving and cold bonding.

The strength value ranging from 30 to 80 MPa can be easily achieved in the lightweight concrete [6-11]. However, the lightweight concrete with the strength ranging between 20 and 50 MPa may be practically produced by using such aggregates [12-16]. The compressive strength, however, is not the only major concept for the structural concretes. The other properties of conventional concrete such as mechanical, permeability and fracture are distinctly different from lightweight concrete. Such properties of lightweight concrete depend on the lightweight aggregate source and manufacturing process. For this reason, each specification of lightweight concrete should be investigated independently for each type of lightweight aggregate concrete [17,18].

This study aims to investigate the fracture and permeability properties of concretes produced at three different water-to-cement (w/c) ratios of 0.35, 0.45, and 0.55 and designated cement contents of 500, 450 and 400 kg/m3, respectively. Artificial fly ash aggregate (AFA) from cold bonding pelletization of FA and PC, and artificial slag aggregate (ASA) from cold bonding pelletization of GGBFS and PC were utilized as coarse aggregate in the concrete production. The AFA and ASA were replaced with natural

aggregate (NA) as 100% of coarse aggregate volume. Namely, three different concrete mixtures were produced at each w/c ratio. Totally, 9 concrete mixtures were produced in this research. The permeability properties of mixtures were investigated in terms of sorptivity, water penetration, gas permeability, and chloride penetration tests whereas the fracture characteristic of the mixtures was investigated with regard to fracture energy test. Moreover, the compressive, splitting tensile and net flexural strength, and modulus of elasticity of concretes were determined. All tests were carried out after 28-day water curing period.

Experimental study

Materials

The portland cement (PC) with specific gravity of 3.15 and Blaine fineness of 394 m2/kg were used in both production of artificial aggregates and concretes. Class F fly ash (FA) provided from Seyhan Sugözü Thermal Power Plant, located in Turkey, and ground granulated blast furnace slag (GGBFS) were used in the artificial aggregate production. FA and GGBFS had the specific gravity of 2.25 and 2.79, and Blaine fineness of 287 and 418 m2/kg, respectively. The physical properties and chemical compositions of PC, FA and GGBFS are given in Table 1. Fine aggregate was the mixing of 20% of crushed limestone sand and 80% of river sand by weight, and the coarse aggregate was the river gravel. They were obtained from natural source. The specific gravity of crushed limestone sand, river sand and river gravel was 2.43, 2.65 and 2.71, respectively. Their physical properties and sieve analysis results are presented in Table 2. Commercially available superplasticizer, Daracem 200, which is sulphaneted naphthalene formaldehyde based, with specific gravity of 1.22 was used to achieve specified slump value for ease of handling, placing and consolidation in all concrete mixtures. The superplasticizer content was adjusted at the time of mixing to achieve target slump value.

Table 1: Chemical compositions and physical properties of Portland cement (PC), fly ash (FA) and ground granulated blast furnace slag (GGBFS)

Chemical analysis (%)	PC	FA	GGBFS
CaO	62.12	4.24	34.12
SiO_2	19.69	56.2	36.41
Al_2O_3	5.16	20.17	10.39
Fe_2O_3	2.88	6.69	0.69
MgO	1.17	1.92	10.26
SO_3	2.63	0.49	-
K_2O	-	1.89	0.97
Na_2O	0.17	0.58	0.35
Loss on ignition	0.87	1.78	1.64

Table 2: Sieve analysis and physical properties of natural and artificial lightweight aggregates

Sieve size (mm)	Natural aggregate (%)			Artificial aggregate (%)	
	Crushed limestone sand	River sand	River gravel	Fly ash aggregate	Slag aggregate
31.5	100	100	100	100	100
16	100	100	100	100	100
8	100	100	42.0	28.1	44.7
4	100	100	0	0	0
2	75.5	68.3	0	0	0
1	53.1	44.6	0	0	0
0.5	32.6	24.8	0	0	0
0.25	21.8	8.7	0	0	0
Specific gravity	2.43	2.65	2.71	1.77	2.28

Concrete mixture proportioning

To investigate the effect of artificial aggregate and w/c ratio, a total of 9 different concrete mixtures were designed. Three cement contents of 500, 450, and 400 kg/m^3 were designated for w/c ratios of 0.35, 0.45, and 0.55, respectively. The artificial aggregates were used as coarse aggregate and the natural coarse aggregate were replaced with artificial aggregate as 100% of total coarse aggregate volume. Mix proportions for 1 m3 concrete are given in Table 3. In mix ID, W denotes the water-to-cement ratio while NA, AFA, ASA represent the natural aggregate, artificial fly ash aggregate, and artificial slag aggregate, respectively. For instance, W35NA indicates that the concrete mixture is designed at water-to-cement ratio of 0.35 with natural aggregate.

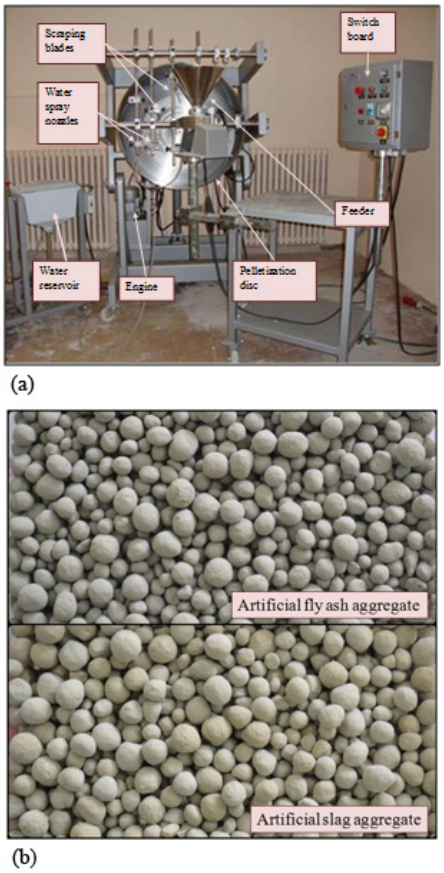

Figure 1: Views of a) General view of pelletization disc and b) artificial fly ash and slag pellets

Table 3: Mix proportions for 1 m3 concrete (kg)

Mix ID	w/c ratio	Cement	Water	Crushed limestone sand	River sand	River gravel	AFA*	ASA*	SP*
W35NA	0.35	500	175.0	158.0	689.1	880.9	0	0	8.5
W35AFA		500	175.0	158.0	689.1	0	575.4	0	8.5
W35ASA		500	175.0	158.0	689.1	0	0	741.1	8.5
W45NA	0.45	450	202.5	155.3	677.5	866.0	0	0	6.0
W45AFA		450	202.5	155.3	677.5	0	565.6	0	6.0
W45ASA		450	202.5	155.3	677.5	0	0	728.6	6.0
W55NA	0.55	400	220.0	155.1	676.4	864.6	0	0	3.0
W55AFA		400	220.0	155.1	676.4	0	564.7	0	3.0
W55ASA		400	220.0	155.1	676.4	0	0	727.4	3.0

*AFA: Artificial fly ash aggregate, ASA: Artificial slag aggregate, SP: Superplasticizer

Specimen preparation and curing

All concrete mixtures were mixed in power-driven revolving pan mixer with capacity of 30 liter. The standard mixing procedure was followed for the concrete mixture with natural aggregate. However, the following special procedure for batching and mixing were followed for the concrete mixture producing with artificial aggregates. Before each mixing, sufficient amount of artificial aggregates were immersed in water for 30 min for saturation. Then, the artificial aggregates were taken out of water and put on the mesh for the outflow of excessive surface water for about 30 s. The extra water on the surface of the pellets (aggregate grains) was rubbed out manually by a dry towel. This is an effective way to obtain SSD condition for the artificial aggregates [16, 20-22]. The SSD aggregate and cement were poured and mixed in the mixer. Then, fine aggregate was added on the aggregate-cement mixture. Water and superplasticizer were mixed before pouring into the mixer. After adding the water, the mixture was mixed for 5 min. As soon as mixing was finished, the slump test was performed and the slump value of 15±2 cm was achieved by adjusting the amount of superplasticizer. As an end, concrete were poured into the moulds with vibration for a couple of seconds. After the concrete casting, all moulded specimens (150-mm cubes, Φ100x200-mm cylinders, Φ150x300-mm cylinders, and 100x100x500-mm prisms) were wrapped with plastic sheet and left in the casting room for 24 h at 20±2 °C and then they were demoulded and 28-day water curing period was applied. Afterwards they were tested based on the testing procedures below.

Testing procedures

ASTM C39 [23] was followed to determine the compressive strength of the concretes for this 150-mm cube specimens were used. Static modulus of elasticity was determined per ASTM C469 [24] on 150-mm cylinder specimens after loading and unloading three times up to 40% of the ultimate load determined from the compression test. The first set of readings from each cylinder was discarded and the elastic modulus was reported as the average of the other two sets of readings. Splitting tensile strength was tested using 100-mm cylinder specimens with respect to ASTM C496 [25] and following expression was used for its calculation:

$$f_s = \frac{2P}{\pi h \Phi} \qquad (1)$$

where P, h, and Φ are the maximum load, length and diameter of the cylinder specimen, respectively.

Fracture energy was determined using 100x100x500-mm prismatic specimens according to the recommendation of RILEM 50-FMC Technical Committee [26]. A closed-loop testing machine with a capacity of 250 kN was used to apply the load. The test set-up and details of the specimen are shown in Fig. 2a and 2b. The notch to depth ratio (a/D) of the specimens was 0.4 and the notch opened by sawing in order to accommodate large aggregates in more abundance reduced the effective cross section to 60x100 mm. Distance between supports was 400 mm and the midspan deflection (δ) was measured by a linear variable displacement transducer (LVDT). Load versus deflection curve was obtained for each specimen and the area under the curve (Wo) was used in the determination of the fracture energy by using following expression given by RILEM 50-FMC Technical Committee [26].

$$G_F = \frac{W_o + mg\frac{S}{U}\delta_s}{B(W-a)} \qquad (2)$$

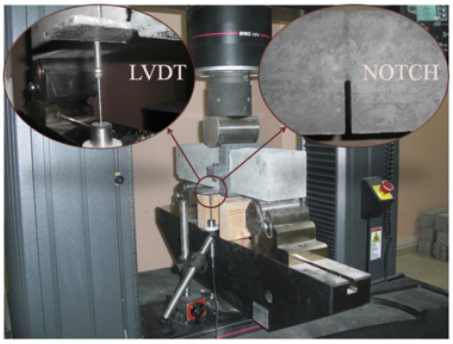

(a)

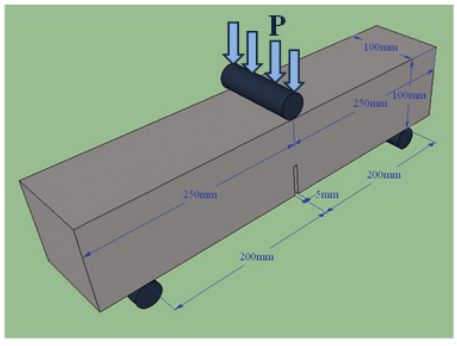

(b)

Figure 2: Views of a) experimental setup for three point bending test and b) dimensions of the notched beam specimen

where B, W, a, S, U, m, δs, and g are the width of the beam, depth of the beam, depth of the notch, span length of the beam, length of the beam, mass of the beam, specified deflection of the beam and gravitational acceleration, respectively. The beams were loaded at a constant rate of 0.02 mm/min. Moreover, the notched beams were used to calculate the net flexural strength by the following equation on the assumption that there is no notch sensitivity, where Pmax is the ultimate load.

$$f_{flex} = \frac{3P_{max}S}{2B(W-a)^2} \qquad (3)$$

Sorptivity test which measures the rate of water drawn into the capillary pores of concrete was carried out after the specimens were dried in an oven at 100±5 °C till they reached the constant mass. The sides of the 50-mm disk specimens cut from 100-mm cylinders were coated by paraffin to prevent water suction from the sides of the specimen. The test was conducted on the surface of concrete that was in contact with water as shown in Fig. 3. The specimens were removed from the tray and weighed at different time intervals up to 1 h to evaluate mass gain. The volume of absorbed water was calculated by dividing the mass gained by nominal surface area of the specimen and by the density of water. Then, the square root of time versus these values was plotted and the sorptivity coefficient (index) of concretes was determined by the slope of the line of the best fit.

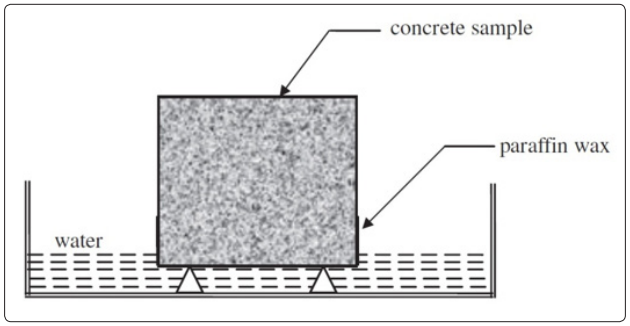

Figure 3: Detail of sorptivity measurement

The water permeability of concretes was measured using 150-mm cubes with respect to TS EN 12390-8 [27]. A 500 ± 50 kPa downward pressure was assigned on the specimens for 72 hours. After 72 hours, the specimens were split from the center point. Then, the largest penetration depth of water is measured in mm. When the concrete likely to come in contact with moderately aggressive media, the water does not penetrate to a depth of more than 50 mm whereas the water penetration depth is not more than 30 mm if concrete is likely to come in touch with aggressive media. A photographic view of the water permeability test equipment is given in Fig. 4a, and typical split specimen and measurement are illustrated in Fig. 4b, 4c, and 4d for concretes produced with NA, AFA, and ASA, respectively.

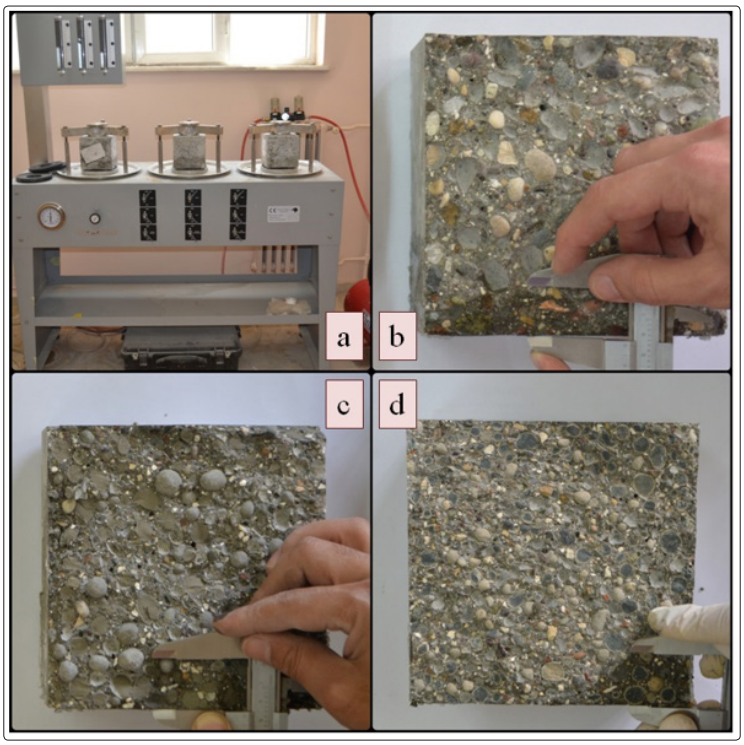

Figure 4: Views: a) Water penetration test device and measurement of penetration depth in: b) normal aggregate, c) artificial fly ash aggregate, and d) artificial slag aggregate concretes

The CEMBUREAU method recommended by RILEM was used to investigate the gas permeability of the concretes. The photographic view and the schematic representation as well as detail of the testing cell are demonstrated in Fig. 5a and 5b, respectively. Oxygen gas was utilized as the permeating medium. The gas permeability coefficients were determined by applying the inlet gas pressures varying from 150 to 500 kPa. Apparent gas permeability coefficient of concrete is average of these coefficients as recommended by RILEM [28]. After 28-day water curing period, the specimens used for the measuring of gas permeability coefficient were dried in oven and at each 6 hours the specimens were weighed till weight change was less than 1%. Then, they were kept in a sealed box till testing. Two disk specimens cut from the mid-portion of 150-mm cylinders were tested at the age of 28 days and the average of them was reported as a test result.

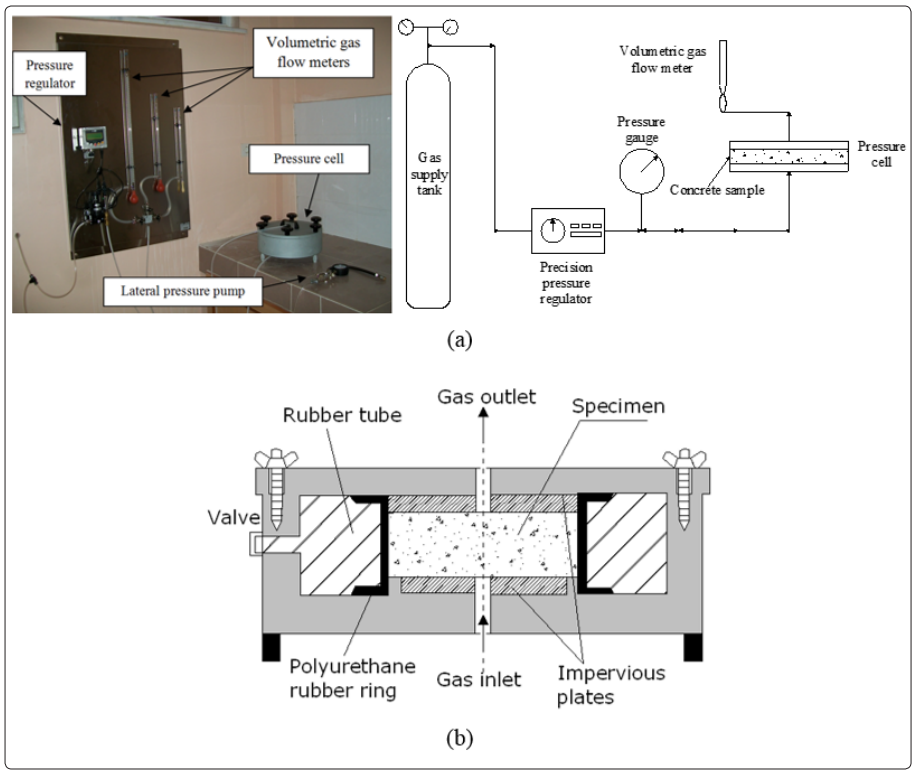

Figure 5: Details of a) gas permeability test set-up and b) pressure cell with test specimen

For each differential pressure (from 150 to 500 kPa), Hagen-Poiseuille relationship for laminar flow of a compressible fluid through a porous media with small capillaries under steady-state condition was used to determine the apparent gas permeability coefficient Kg, which can be calculated using the modified Darcy's equation:

$$K_g = \frac{2P_2QL\mu}{A(P_1^2 - P_2^2)} \quad (2)$$

where Kg is the gas permeability coefficient (m^2), P1 is the inlet gas pressure (N/m^2), P2 is the outlet gas pressure (N/m^2), A is the cross-sectional area of the sample (m^2), L is the height of sample (m), μ is the viscosity of oxygen ($2.02x10^{-5}$ Ns/m^2), and Q is the volume flow rate (m^3/s).

The resistance to the penetration of the chloride ions was measured in terms of the charge passed through concrete in accordance with ASTM C1202 [29]. To avoid variations induced by bleeding and repetitive vibration, three 50-mm disk specimens were cut from the mid-portion of each Ø100x200-mm cylinder specimen, soon after 28-day water curing period. The samples were conditioned as mentioned in ASTM C1202. Then, the disk specimens were placed in the test cell where one surface of the specimen was in touch with 0.3 N sodium hydroxide (NaOH) solution and the other surface with 3% sodium chloride (NaCl) solution. A direct current of 60 ± 0.1 volts was applied across the specimen faces, and the current across the specimen was recorded, covering a total period of 6 h. By knowing the current and time history, the total charge (coulombs) passed through the specimen was computed by Simpson's integration. The results presented are the averages from three concrete specimens.

Results and discussion

Compressive strength and modulus of elasticity

The 28-day compressive strength versus the water cement ratio (w/c) of concretes with NA, AFA, and ASA is given in Fig. 6. The lowest compressive strength value of 31.46 MPa was determined at W55AFA while the maximum value of 63.1 MPa was measured at W35ASA. The compressive strength values varying between 45.6 and 63.1 MPa was obtained for the concretes produced at w/c ratio of 0.35, while the compressive strength range of concretes were between 34.8 and 50.2 MPa at w/c ratio of 0.45, and between 31.4 and 44.8 MPa at w/c ratio of 0.55. At each w/c ratio, the highest compressive strength values were obtained in the concretes produced with ASA, while the lowest compressive strength values were obtained in the concretes produced with AFA. Since the AFA is relatively weaker than NA, replacing NA with AFA caused a lower compressive strength. However, the ASA was more strength than the AFA and also, the utilization of ASA in the concrete production resulted in pozzolanic reaction between the paste and aggregate. This is also known as secondary reaction that is between calcium from portlandite and the dissolved minerals resulting from the cold bonding agglomeration process of GGBFS. Secondary reaction enhanced the cement paste in the concrete and resulted in higher compressive strength of ASA concrete compared to NA concrete. As a result, replacing the NA with AFA decreased the compressive strength as much as 22.2, 23.0, and 18.7% at w/c ratios of 0.35, 0.45, and 0.55, respectively, whereas replacing the NA with ASA increased the compressive strength as much as 7.7, 11.1, and 16.1% at w/c ratios of 0.35, 0.45, and 0.55, respectively. Moreover, the effect of w/c ratio on compressive strength was also investigated and results indicated that reducing the w/c ratio increases the compressive strength of each type of concrete systematically.

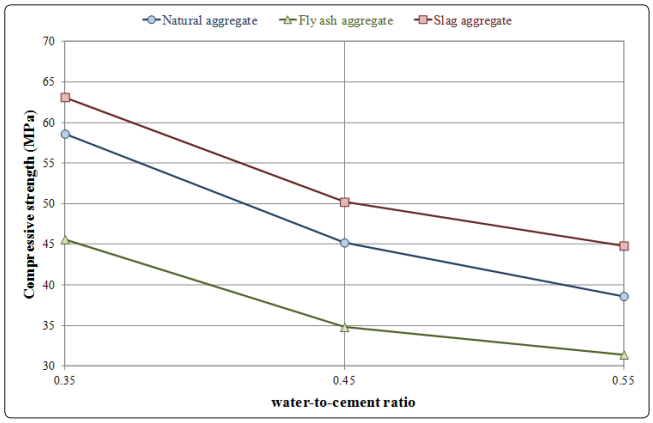

Figure 6: Variations in the compressive strength of NA, AFA, and ASA concretes with water-to-cement ratio

Variations in static modulus of elasticity versus w/c ratio of NA, AFA, and ASA concretes are presented in Fig. 7. The modulus of elasticity values ranging between 19.7 and 39.8 GPa were achieved in this study. The highest modulus of elasticity values were determined in the concretes produced with ASA, while the lowest values were measured in the concretes produced with AFA at each w/c ratio. As expected, decreasing the w/c ratio resulted in increasing the modulus of elasticity of not only for NA concretes but also AFA and ASA concretes.

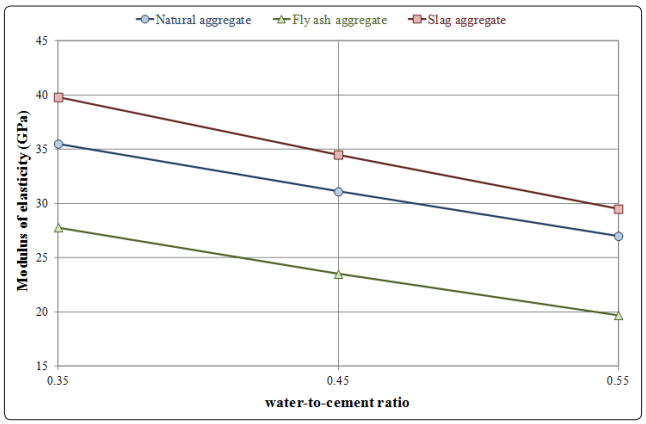

Figure 7: Variations in the modulus of elasticity of NA, AFA, and ASA concretes with water-to-cement ratio

In addition, the analysis of variance (ANOVA) was used to find out that whether an independent variable has an effect on dependent variable or not. The effectiveness of the test parameters was determined by the general linear model analysis of variance (GLM-ANOVA) which is an important statistical analysis and diagnostic tool which helps to quantify the dominance of a control factor by reducing the control variance. The mechanical properties such as the compressive strength, the modulus of elasticity, the splitting tensile and the net flexural strengths, as well as the fracture energy, and the permeability properties such as the sorptivity index, the water penetration, the resistance to chloride penetration in terms of rapid chloride permeability test (RCPT), and apparent gas

permeability coefficient of concretes were analyzed separately and assigned as dependent variable while the aggregate type and w/c ratio were selected as independent factors. The software called Minitab used to analyze the test results obtained from this study and the analysis was carried out at a 0.05 level of significance to specify the statistically significant experimental parameters on the mechanical, fracture and permeability characteristics of concretes. The statistical analysis results achieved from GLM-ANOVA are presented in Table 4. The P-values in the sixth columns show the significance of the test parameters on such properties. P-value less than 0.05 means that the parameter is acceptable as a significant factor on the test result. Besides, percent contribution was also determined to have an idea about the degree of effectiveness of each independent variable on the dependent variable. When the percent contribution of one parameter, which was calculated by the division of sequential sum of squares of independent variable to total sequential sum of squares of each dependent variable, is higher, the effectiveness of that parameter on the analyzed property is higher. Likewise, if the percent contribution is low, the contribution of the factors to that particular response is less.

According to the statistical evaluation, it can be concluded that aggregate type and w/c ratio has significant effect on the compressive strength and the modulus of elasticity of concretes. Moreover, when the percent contribution given in eighth column of Table 4 was considered, it can be seen that the compressive strength was affected by both aggregate type and w/c ratio with near percent contribution values while the modulus of elasticity was affected by aggregate type with percent contribution value of 60.6% more than w/c ratio with percent contribution value of 38.9%.

Table 4: Statistical evaluation of performance characteristics of concretes

Dependent variable	Independent variable	Sequential sum of squares	Computed F	R-square (%)	P value	Significance	Contribution (%)
Compressive strength	Aggregate type	369.616	82.71	98.97	0.001	Yes	42.8
	w/c ratio	485.536	108.65		0.000	Yes	56.2
	Error	8.938	-		-	-	1.0
	Total	864.089	-		-	-	-
Modulus of elasticity	Aggregate type	187.849	272.68	99.56	0.000	Yes	60.6
	w/c ratio	120.669	175.16		0.000	Yes	38.9
	Error	1.378	-		-	-	0.5
	Total	309.896	-		-	-	-
Splitting tensile strength	Aggregate type	0.33662	39.50	99.15	0.002	Yes	16.8
	w/c ratio	1.64869	193.46		0.000	Yes	82.3
	Error	0.01704	-		-	-	0.9
	Total	2.00236	-		-	-	-
Fracture energy	Aggregate type	5739.23	521.12	99.72	0.000	Yes	73.7
	w/c ratio	2028.53	184.19		0.000	Yes	26.0
	Error	22.03	-		-	-	-
	Total	7789.78	-		-	-	-
Net flexural strength	Aggregate type	1.99500	260.22	99.45	0.000	Yes	71.3
	w/c ratio	0.78847	102.84		0.000	0.000	28.2
	Error	0.01533	-		-	-	0.5
	Total	2.79880	-		-	-	-
Soprtivitiy index	Aggregate type	0.0068802	14.19	95.90	0.015	No	29.1
	w/c ratio	0.0157929	32.57		0.003	Yes	66.8
	Error	0.0009698	-		-	-	4.1
	Total	0.0236429	-		-	-	-
Water penetration	Aggregate type	113.167	159.76	99.34	0.000	Yes	52.5
	w/c ratio	101.167	142.82		0.000	Yes	46.9
	Error	1.417	-		-	-	0.6
	Total	215.750	-		-	-	-
Apparent gas permeability	Aggregate type	1.39842	168.03	99.56	0.000	Yes	37.3
	w/c ratio	2.33162	280.17		0.000	Yes	62.2
	Error	0.01664	-		-	-	0.5
	Total	3.74669	-		-	-	-

Rapid chloride permeability	Aggregate type	2232214	17.91	98.97	0.010	No	9.3
	w/c ratio	21634972	173.58		0.000	Yes	89.7
	Error	249284	-		-	-	1.0
	Total	24116470	-		-	-	-

Splitting tensile strength

The splitting tensile strength of the concretes is presented in Fig. 8. The lowest splitting tensile strength value of 2.33 MPa was determined at W55AFA whereas the maximum value of 3.75 MPa was measured at W35NA. The highest splitting tensile strength results were obtained in the concrete produced with NA, while the lowest results were gotten in the concrete manufactured with AFA. The replacing the NA with AFA decreased the splitting tensile strengths about 13.3, 16.3, and 15.0% and the substituting the NA with ASA decreased the splitting tensile strengths about 3.5, 7.7, and 10.6% at w/c ratios of 0.35, 0.45, and 0.55, respectively. Although use of ASA in the concrete production increased the compressive strength of concrete, the same effect in splitting tensile strength was not observed. It may be explained as the ASA enhanced the cement paste with secondary reaction that occurs between calcium from portlandite and the dissolved minerals resulting from the cold bonding agglomeration process of GGBFS. Therefore, the ASA using increased the compressive strength since compressive loads are carried by both cement paste and aggregate. However, the aggregates are responsible for carrying the tensile loads in concrete. For this reason, utilization of weak aggregates, such as AFA and ASA, in concrete production resulted in lower splitting tensile strength. Additionally, the statistical evaluation indicated that both aggregate type and w/c ratio have remarkable effect on splitting tensile strength when the p-values were considered. The percent contribution value of w/c ratio was 82.3%, while that of aggregate type was about 16.8% (Table 4). The high percent contribution of w/c ratio means that the effectiveness of this parameter on the splitting tensile strength is high.

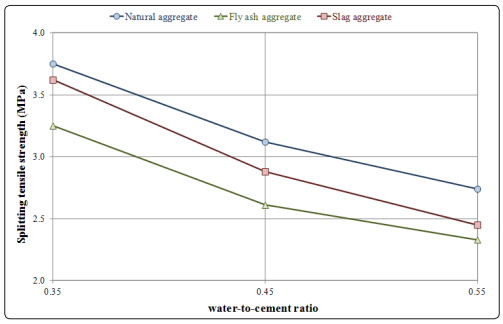

Figure 8: Variations in the splitting tensile strength of NA, AFA, and ASA concretes with water-to-cement ratio

Fracture energy and net flexural strength

The variations in fracture energy versus w/c ratios of NA, AFA, and ASA concretes are illustrated in Fig. 9. The fracture energies of concretes produced with natural aggregate at w/c ratio of 0.35, 0.45, and 0.55 are 145.1, 124.1, and 107.8 N/m, respectively. Utilization of artificial aggregates decreased the fracture energies of concrete at each w/c ratio. In the calculation of fracture energy the area under the load versus displacement curve was used as an indication of the energy supplied by the actuator, and the weight of the beam was used as the energy supplied by the own weight of the beam. The concretes produced with NA at each w/c ratio gave higher area under the load versus displacement curve in contrast to concretes produced with AFA and ASA as can be clearly seen in Fig. 10a, 10b, and 10c. It means that concretes produced with NA had higher load carrying capacity when they subjected to three-point bending load than that produced with AFA and ASA. Apart from this, the concretes produced with NA and ASA performed same average maximum displacement of 1.5 mm at each w/c ratio while the average maximum displacements of concretes produced with AFA at w/c ratios of 0.35, 0.45, and 0.55 were about 0.91, 0.86, and 0.80 mm, respectively. Fig. 10a, 10b, and 10c represent the typical load versus displacement curves of NA, AFA, and ASA concretes at w/c ratio of 0.35, 0.45, and 0.55, respectively. Furthermore, statistical evaluation demonstrated that both aggregate type and w/c ratio has significant effect on fracture energy according to p-values but the effectiveness of aggregate type on fracture energy is higher than that of w/c ratio when the percent contribution values are considered.

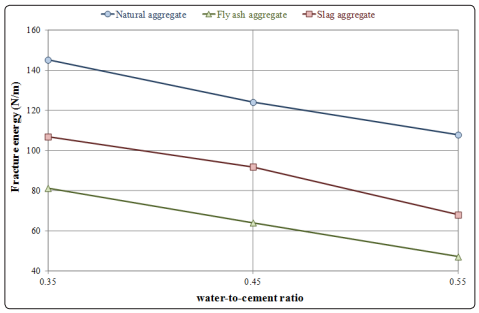

Figure 9: Variations in the fracture energy of NA, AFA, and ASA concretes with water-to-cement ratio

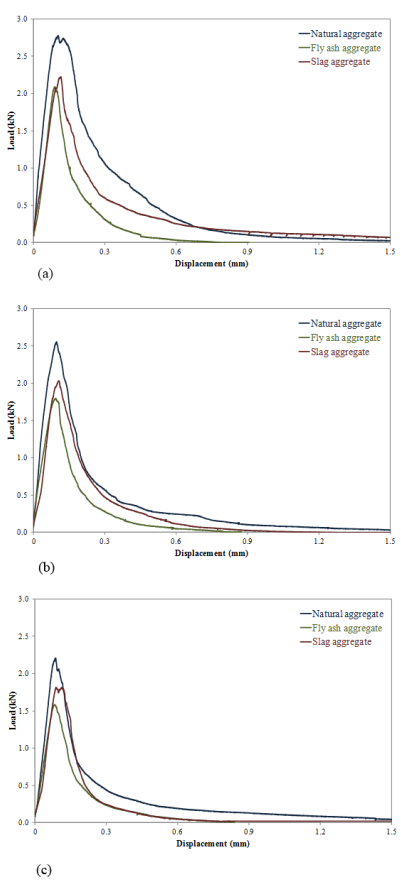

Figure 10: Load vs. displacement curves for NA, AFA, and ASA concretes at w/c ratios of: a) 0.35, b) 0.45, and c) 0.55

The net flexural strengths of concretes obtained from notched prismatic specimens subjected to three-point bending test are presented in Fig. 11. The similar effect of artificial aggregate as in the splitting tensile strength was observed in net flexural strength. Utilization of AFA and ASA aggregate decreased the net flexural strength. The concretes manufactured with NA had the net flexural strength values of 4.42, 3.91, and 3.68 MPa at w/c ratios of 0.35, 0.45, and 0.55, respectively. Replacing the NA with the AFA and ASA decreased the net flexural strength as much as 26.0, 29.9, and 30.8%, and 16.4, 13.9, and 18.5% at w/c ratios of 0.35, 0.45, and 0.55, respectively. The results also revealed that decreasing the w/c ratio significantly increased the net flexural strength of concretes. In addition to these, remarkable effect of aggregate type and w/c ratio on net flexural strength with respect to p-values was seen by statistical analysis (Table 4). When the percent contributions of aggregate type and w/c ratio were considered, it can be said that aggregate type is more effective than w/c ratio in the net flexural strength.

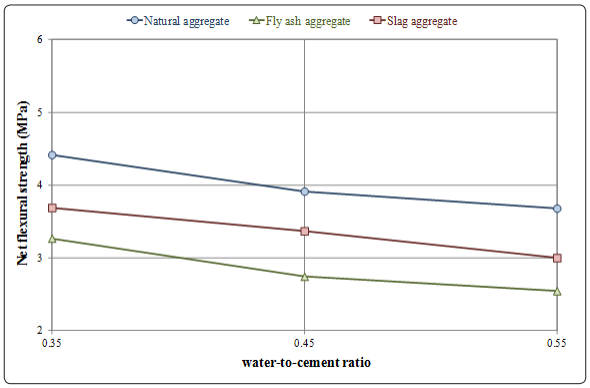

Figure 11: Variations in the net flexural strength of NA, AFA, and ASA concretes with water-to-cement ratio

Water sorptivity

The 28-day sorptivity coefficients for concretes produced with NA, AFA, and ASA are given in Fig. 12. The concretes manufactured with natural aggregate performed better than that produced with AFA and ASA. Decreasing the w/c ratio significantly improved the water sorptivity characteristic of concretes since the cement paste is enhanced by decreasing the w/c ratio. Reduced sorptivity reflects a finer pore structure that would, for example, inhibit ingress of aggressive elements into the system [30]. Therefore, minimizing sorptivity is important in order to reduce the ingress of chloride-containing or sulfate-containing water into concrete, which can cause serious damage [31]. Sorptivity coefficients of 0.114, 0.14 and 0.204 mm/mm$^{0.5}$ were obtained in the concrete produced with NA at w/c ratios of 0.35, 0.45, and 0.55, respectively. However, the replacing the NA with the AFA caused an increasing in the sorptivity coefficients about 48.2, 36.4, and 45.6%, whereas the substituting the NA with the ASA caused an increasing in the sorptivity coefficients about 24.6, 15.7, and 6.9% at w/c ratios of 0.35, 0.45, and 0.55, respectively. This circumstance can be explained by high water absorption of artificial aggregates, since the 24-hour water absorption of the AFA and ASA were 20.8 and 7.5% while that of the NA was about 1.4%. The higher water absorption of aggregate resulted in higher sorptivity coefficient. Besides, statistical analysis indicated that the percent contribution of w/c ratio is higher than that of aggregate type (Table 4). It means that the w/c ratio is more effective than aggregate type on sorptivity index.

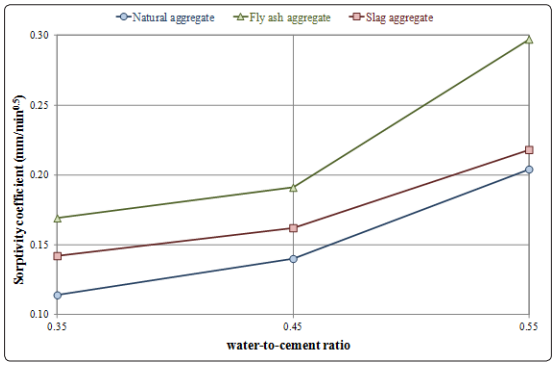

Figure 12: Effect of aggregate type and w/c ratio on the sorptivity coefficient of concretes

Gas permeability

The behavior of concrete produced at w/c ratio of 0.35, 0.45, and 0.55 are respectively illustrated in Fig. 14a, 14b and 14c according to the inlet pressure head. The apparent gas permeability coefficients of the concretes produced with NA, AFA, and ASA were varied with the inlet pressure from 150 to 500 kPa. The apparent gas permeability was calculated on the basis of the Hagen-Poiseuille relationship for laminar flow of a compressible fluid through a porous body with small capillaries under steady-state conditions [32]. There is a tendency of the gas permeability coefficient to diminish up to 350 kPa and then to rise after the inlet pressure of 350 kPa till 500 kPa. Both AFA and ASA concretes had higher values of permeability coefficient than that of NA concretes at each w/c ratio.

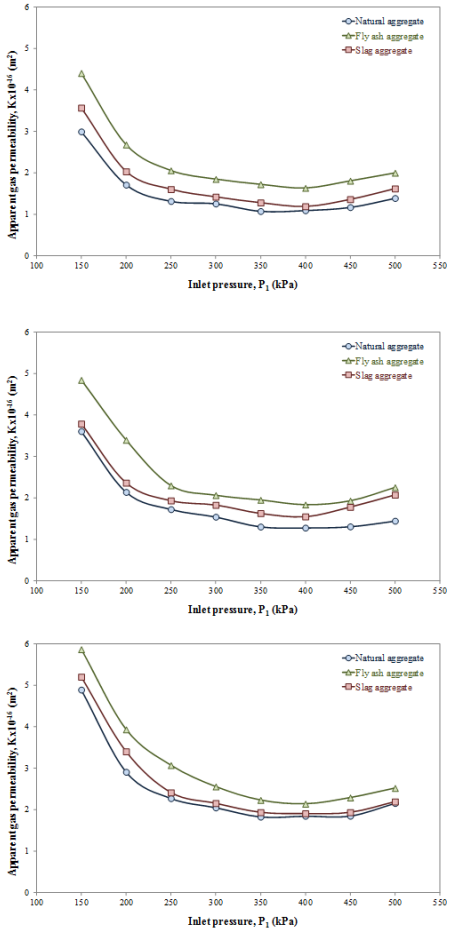

Figure 14: Variations in apparent gas permeability versus inlet pressure for NA, AFA, and ASA concretes at water-to-cement ratios of: a) 0.35, b) 0.45, and c) 0.55

RILEM suggests determining the average gas permeability coefficient by taking the average of the coefficients at 150, 200, 300 kPa inlet pressures [28]. The coefficients of apparent gas permeability determined according to RILEM for concrete produced with NA, AFA, and ASA are given in Fig. 15. The apparent gas permeability coefficients in this study ranged between 1.99-2.98x10^{-16} m^2, 2.43-3.43x10^{-16} m^2, and 3.28-4.12x10^{-16} m^2 for concrete designed at w/c ratio 0.35, 0.45, and 0.55, respectively. As can be seen from the Fig. 13d, decreasing the w/c ratio increase the gas permeability resistance of concretes. Substituting the NA with ASA in concrete production performed better resistance than replacing the NA with AFA in concrete production at each w/c ratio. Besides, the statistical analysis indicated that gas permeability characteristic of concretes are remarkably affected by aggregate type and w/c ratio when p-values were considered. According to the percent contribution of aggregate type and w/c ratio, it can be said the effective parameter on apparent gas permeability coefficient is w/c ratio with the percent contribution value of 62.2%.

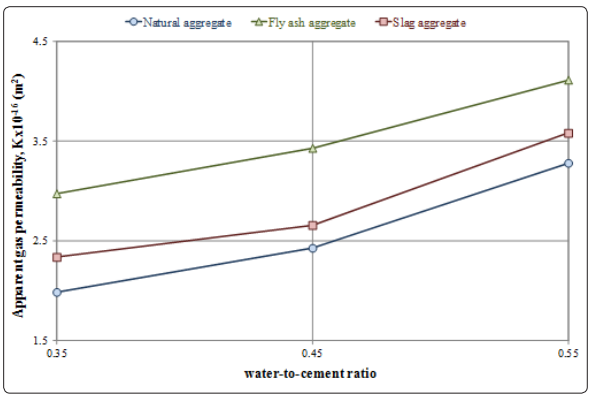

Figure 15: Effect of aggregate type and w/c ratio on apparent gas permeability of concretes

Resistance to chloride ion penetration

The resistance of concretes to chloride ion penetration was measured according to rapid chloride permeability test (RCPT). The results obtained from this test are determined as the total charge passed and presented in Fig. 16. The lowest total charge passed of 3276 C was measured at W35NA while the maximum of 7933.3 C was measured at W55AFA. The mix W35NA and W35ASA can be considered as "moderate" according to the classification of concretes for chloride permeability, while the other mixes are classified as "high" chloride permeability rating (Table 5). The AFA and ASA utilization in concrete production decreased the concrete resistance to chloride ion penetration. Due to the fact that the concretes produced in this study generally were in "high" chloride permeability class according to ASTM C1202 [29], it may be proposed that the utilization of these concretes are more suitable for the structures having no risk of severe chloride attack. In addition, statistical evaluation revealed that the w/c ratio is more effective parameter than aggregate type on resistance to chloride ion penetration when percent contributions were regarded (Table 4).

Discussion

Based on the findings presented in this study, the following conclusions can be drawn:

- The greatest compressive strength values were obtained in the concretes produced with ASA at each w/c ratio. Decreasing the w/c ratio increased the compressive strength of concretes. Besides, the modulus of elasticity ranging between 19.7 and 35.5 GPa were determined and the greatest modulus of elasticity values of concrete were measured in concrete with ASA while the lowest modulus of elasticity values were determined in concrete with AFA at each w/c ratio.
- The splitting tensile strength values ranging between 2.33 and 3.75 MPa were achieved in this study. The highest splitting tensile strengths were obtained in the concretes produced with NA at each w/c ratio. The results indicated that utilization of weak aggregate in concrete production caused a decreasing in splitting tensile strength.
- The fracture energy and net flexural strength were determined in this study by using notched beams. The results demonstrated that decreasing the w/c ratio increased both fracture energy and net flexural strength. Additionally, the lowest fracture energy and net flexural strength were measured in the concretes manufactured with AFA. Besides, the concretes produced with AFA performed the lower displacement while the concrete produced with NA and ASA gave the same displacement of 1.5 mm.
- The water sorptivity of concretes were also measured and the sorptivity coefficients ranging between 0.114 and 0.297 mm/mm0.5 were measured. Utilization of aggregates, which has high water absorption, increased the sorptivity coefficients of concrete. Also, increasing the w/c ratio increased the sorptivity coefficient of concrete produced with NA, AFA, and ASA.
- The water penetration depths of concretes were measured and it was revealed that the concrete produced with lower w/c ratio performed better resistance to water permeability. The concretes produced with AFA and ASA gave higher water penetration depth than that produced with NA since artificial aggregates are weak and have micro and macro porosities in its structure.
- The results indicated that the concretes manufactured at lower w/c ratio performed better resistance to gas permeability. Moreover, it was noticed that utilization of artificial aggregate increased the gas permeability of both AFA and ASA concrete. However, ASA concretes at each w/c ratio performed better gas permeability characteristic than AFA concretes.
- Resistance to chloride ion penetration was measured by using rapid chloride permeability test and the results obtained from this study were used to determine the total charge passed. W35NA and W35ASA can be considered as "moderate" class according to classification given by ASTM C1202 while the remained concrete mixtures are classified as "high" class.
- The statistical analysis results indicated that all investigated properties of concrete were significantly affected by the aggregate type and the w/c ratio regarding the P-values obtained from the two-way ANOVA. The statistical analysis also revealed that such dependent parameters, the compressive strength, the splitting tensile strength, water sorptivity, gas permeability, and resistance to chloride ion penetration were more influenced by the w/c ratio than aggregate type when the percent contribution values of independent variables were considered.

References

1. Safiuddin MD, Salam MA, Jumaat MZ (2011) Effects of recycled concrete aggregate on the fresh properties of self-consolidating concrete. Arc Civ Mech Eng 11:1023-1041.
2. Khaleel OR, Al-Mishhadan SA, Razak HA (2011) The effect of coarse aggregate on fresh and hardened properties of self-compacting concrete (SCC). Procedia Eng 14:805-813.
3. Zhang MH, Gjorv OE (1991) Characteristics of lightweight aggregates for high strength concrete. ACI Mater J 88:150-158.

4. Turkish Statistical Institute, Press Release 8, 2010, http://www.turkstat.gov.tr/.
5. Bilgen G, Kavak A, Yıldırım ST, Çapar OF. Blast furnace slag and its importance in the construction sectors, in: 578 The Second National Solid Waste Management Conference, Mersin, Turkey, 2010.
6. Zhang MH, Gjorv OE (1991) Mechanical properties of high strength lightweight concrete. ACI Mater J 88:240-247.
7. Videla C, Lopez M (2000) Mixture proportioning methodology for structural sandlightweight concrete. ACI Mater J 97:281-289.
8. Haque N, Lopez M (1999) Strength and durability of lightweight concrete in hot marine exposure conditions. Mater Struct 32:533-538.
9. Al-Khaiyat H, Haque N (1999) Strength and durability of lightweight and normal weight concrete. J Mater Civil Eng 11:231-235.
10. Khaloo AR, Kim N (1999) Effect of curing condition on strength and elastic modulus of lightweight high-strength concrete. ACI Mater J 96:485-90.
11. Haque MN, Al-K haiat H, Kayali O (2007) Strength and durability of lightweight concrete. Cement Concr Comp 26:307-314.
12. Chi JM, Huang R, Yang CC, Yang JJ (2003) Effect of aggregate properties on the strength and stiffness of the lightweight concrete. Cement Concr Comp 25:197-205.
13. Yang CC (1997) Approximate elastic moduli of lightweight aggregate. Cement Concr Res 27:1021-1030.
14. Chang TP, Shieh MM (1996) Fracture properties of lightweight concrete. Cement Concr Res 26:181-188.
15. Gesoğlu M, Özturan T, Güneyisi E (2004) Shrinkage cracking of lightweight concrete made with cold-bonded fly ash aggregates. Cement Concr Res 34:1121-1130.
16. Güneyisi E, Gesoğlu M, İpek S (2013) Effect of steel fiber addition and aspect ratio on bond strength of cold-bonded fly ash lightweight aggregate concretes. Construction and Building Materials 47:358-565
17. Kayali O, Haque MN, Zhu B (1999) Drying shrinkage of fiber-reinforced lightweight aggregate concrete containing fly ash. Cem Concr Res 29:1835-1840
18. Güneyisi E, Gesoğlu M, Booya E (2012) Fresh properties of self-compacting cold bonded fly ash lightweight aggregate concrete with different mineral admixtures. Materials and Structures 45:1849-1859.
19. ASTM C 127. Standard test method for specific gravity and absorption of coarse aggregate, Annual Book of ASTM Standards; 2007.
20. Gesoğlu M. Effects of lightweight aggregate properties on mechanical, fracture, and physical behavior of lightweight concretes. PhD thesis, 2004. Istanbul, Boğaziçi University.
21. Gesoğlu M, Güneyisi E, Öz HÖ (2012) Properties of lightweight aggregates produced with col-bonding pelletization of fly ash and ground granulated blast furnace slag. Materials and Structures 45:1535-1546.
22. Joseph G, Ramamurthy K (2009) Influence of fly ash on strength and sorption characteristics of cold-bonded fly ash aggregate concrete. Const Build Mater 23:1862-70.
23. ASTM C39/C39M-12. Standard test method for compressive strength of cylindrical concrete specimens. Annual book of ASTM Standard; 2012.
24. ASTM C469/C469M−10 (2010) Standard Test Method for Static Modulus of Elasticity and Poisson's Ratio of Concrete in Compression. Book of Standards 4:1-5.
25. ASTM C 496. Standard test method for split tensile strength of cylindrical concrete specimens. Annual Book of ASTM Standards; 1994.
26. RILEM 50-FMC (1985) Committee of fracture mechanics of concrete. Determination of fracture energy of mortar and concrete by means of three-point bend tests on notched beams. Mater Struct 18:285-90.
27. TS EN 12390-8. Testing hardened concrete – Part 8: Depth of penetration of water under pressure. Institute of Turkish Standards, Ankara, Turkey; 2002.
28. Rilem TC 116-PCD (1999) Permeability of concrete as a criterion of its durability. Mater Struct 32:174-179.
29. ASTM C1202 Test method for electrical indication of concrete's ability to resist chloride ion penetration, Annual Book of ASTM Standards; 2006.
30. Chan SYN, Ji X (1998) Water sorptivity and chloride diffusivity of oil shale ash concrete. Constr Build Mater 12:177-183.
31. Chindaprasirt P, Chotithanormc C, Cao HT, Sirivivatnanon V (2007) Influence of fly ash fineness on the chloride penetration of concrete. Constr Build Mater 21:356-361.
32. Kollek JJ (1989) Determination of the permeability of concrete to oxygen by the cembureau method-recommendation. Mater Struct 22:225-230.